Superconductivity in $LaFe_{1-x}Co_xAsO$

Athena S. Sefat,[1] Ashfia Huq,[2] Michael A. McGuire,[1] Rongying Jin,[1] Brian C. Sales,[1] David Mandrus,[1] Lachlan M. D. Cranswick,[3] Peter W. Stephens,[4] and Kevin H. Stone[4]

[1]*Materials Science & Technology Division, Oak Ridge National Laboratory, Oak Ridge, Tennessee 37831, USA*

[2]*Neutron Scattering Science Division, Oak Ridge National Laboratory, Oak Ridge, Tennessee 37831, USA*

[3]*Canadian Neutron Beam Centre, National Research Council, Chalk River, Ontario, Canada K0J 1J0*

[4]*Department of Physics & Astronomy, Stony Brook University, Stony Brook, New York 11794, USA*

(Received 6 July 2008; revised manuscript received 4 August 2008; published 10 September 2008)

Here we report the synthesis and basic characterization of $LaFe_{1-x}Co_xAsO$ for several values of x. The parent phase LaFeAsO orders antiferromagnetically ($T_N \approx 145$ K). Replacing Fe with Co is expected both to electron dope and introduce disorder in the FeAs layer. For $x=0.05$ antiferromagnetic order is destroyed and superconductivity is observed at $T_c^{\text{onset}}=11.2$ K. For $x=0.11$ superconductivity is observed at $T_c^{\text{onset}}=14.3$ K and for $x=0.15$ it is observed at $T_c^{\text{onset}}=6.0$ K. For $x=1$, and the material appears to be ferromagnetic as judged by magnetization measurements. We conclude that Co is an effective dopant to induce superconductivity. Somewhat surprisingly, the system appears to tolerate considerable disorder in the FeAs planes.

DOI: 10.1103/PhysRevB.78.104505 PACS number(s): 74.62.Dh, 74.62.Bf, 74.72.−h, 74.81.Bd

I. INTRODUCTION

The recent reports of $T_c \sim 26$ K in $LaFeAsO_{1-x}F_x$ ($x \sim 0.11$) (Refs. 1–10) and related materials have attracted a great deal of attention as these appear to be unconventional high-T_c superconductors that are based on iron instead of copper. It is interesting to compare and contrast the behavior of the iron arsenide superconductors with the cuprates. For high-T_c copper oxides, the parent compounds are antiferromagnetic Mott insulators[11] and the magnetic order is suppressed and superconductivity emerges by doping with either electrons or holes.[12] Much like copper oxide superconductors, high T_c in the Fe-based family of *R*FeAsO (*R* =rare-earth) is caused by doping. Here is a report of superconductivity in LaFeAsO by electron doping by means of cobalt substitution in the layers of $FeAs_4$ tetrahedra in $LaFe_{1-x}Co_xAsO$ (Fig. 1).

The parent LaFeAsO crystallizes with the ZrCuSiAs-type structure[13] in $P4/nmm$ space group (No. 129; $Z=2$).[14,15] Electronic structure calculations[16] describe the structure as quasi-two dimensional (2D), composed of sheets of metallic Fe^{2+} in between ionic blocks of $LaOAs^{2-}$ along the c axis. Although there is bonding between Fe and As (d =2.3–2.4 Å), the states near the Fermi level are dominated by Fe d states lightly mixed with As p states. LaFeAsO undergoes a continuous or weakly first-order structural phase transition from tetragonal ($P4/nmm$) to orthorhombic ($Cmma$) upon cooling below 155–160 K (Refs. 8, 17, and 18); this is followed by a commensurate antiferromagnetic order just below 135–150 K.[7,8,19] *Ab initio* calculations yield Fe magnetic moments ranging from 1.5 to 2.3 μ_B,[5,20–22] while weak superlattice reflections in neutron scattering[17] and Mössbauer spectra[7,8] indicate a much smaller value of 0.25–0.35 μ_B/Fe.

Carrier doping plays a major role in the appearance of superconductivity by suppressing the magnetic order and structural phase transition in $LaFeAsO_{1-x}F_x$.[7,23,24] Substitution of La for other rare earths (R) has resulted in finding F-doped $RFeAsO_{1-x}F_x$ (R=Pr, Sm, Nd, and Gd) superconductors,[25–30] giving T_c as high as 55 K in $SmFeAsO_{0.9}F_{0.1}$.[30] Th^{4+} doping in $Gd_{1-x}Th_xFeAsO$ gives slightly higher T_c at 56 K.[31] Hole doping, by substituting Sr^{2+} for La^{3+}, results in $T_c=25$ K.[32] A series of oxygen deficient $RFeAsO_{1-\delta}$ give highest $T_c=55$ K for $SmFeAsO_{0.85}$.[33–35] Here we report the synthesis and characterization of Co-doped LaFeAsO and find superconductivity for ~4–12% doping levels. Chemically, Co is a better mean of electron doping as carriers are doped directly into the FeAs planes. This also provides information as to how well the superconductors tolerate in-plane disorder.

For $LaFe_{1-x}Co_xAsO$, experimental details below are followed by a discussion of the crystal structure from powder x-ray and neutron diffractions for ($0 \le x \le 1$). The thermodynamic and transport properties of this material will then be presented and discussed. The measurements include field- and temperature-dependent magnetic susceptibility, electrical resistivity, and Seebeck coefficient.

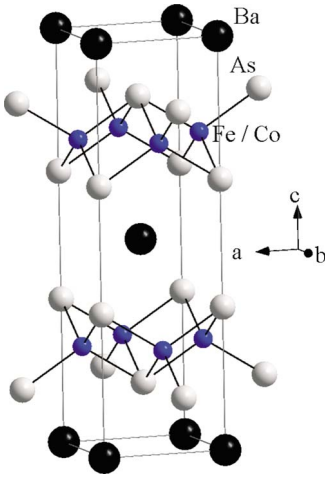

FIG. 1. (Color online) Crystal structure of $LaFe_{1-x}Co_xAsO$ with tetragonal ZrCuSiAs type. It is composed of layers of edge-sharing OLa_4 tetrahedra alternating with layers of Fe(/Co)As_4 along the c axis. The unit cell is represented in gray lines.

TABLE I. Crystallographic data of LaFeAsO.

T (K)	4		300
Space group	*Cmma*		*P*4/*nmm*
a (Å)	5.6823(2)		4.0345(1)
b (Å)	5.7103(2)		$=a$
c (Å)	8.7117(4)		8.7387(4)
V (Å^3)	282.67(2)		142.24(1)
Z	4		2
d range (Å)		0.8–10.6	
wR_p	3.17		3.20
χ^2	7.14		5.92
Atomic parameters:			
La	$4g(0,\frac{1}{4},z)$, z=0.1424(3) U_{iso}=0.0025(8) Å^2		$2c(\frac{1}{4},\frac{1}{4},z)$, z=0.1420(3) U_{iso}=0.0066(11) Å^2
Fe	$4b(\frac{1}{4},0,\frac{1}{2})$, U_{iso}=0.0011(6)		$2b(\frac{3}{4},\frac{1}{2},z)$, U_{iso}=0.0055(8) Å^2
As	$4g(0,\frac{1}{4},z)$, z=0.6501(4) U_{iso}=0.0009(10) Å^2		$2c(\frac{1}{4},\frac{1}{4},z)$, z=0.6498(4) U_{iso}=0.0045(12) Å^2
O	$4a(\frac{1}{4},0,0)$, U_{iso}=0.0049(11) Å^2		$2a(\frac{3}{4},\frac{1}{4},0)$, U_{iso}=0.0096(13) Å^2

II. EXPERIMENTAL DETAILS

Polycrystalline samples with $LaFe_{1-x}Co_xAsO$ (x=0, 0.05, 0.11, 0.15, 0.2, 0.5, and 1) nominal compositions were synthesized by stoichiometrically mixing fine powders of LaAs,[2] Co_3O_4 (99.9985%), Fe_2O_3 (99.99%, calcined at 900 °C for 12 h), and Fe (99.998%), pressing into a pellet, and rapidly heating in silica tubes. The silica tubes were sealed under partial pressure of argon and heated at 1220 °C for ~12 h, then rapidly cooled by shutting off the furnace. Each pellet was reground and reannealed. The source of all elements or compounds was Alfa Aesar.

The initial phase purity and structural identification were made via powder x-ray diffraction using a Scintag XDS 2000 θ-θ diffractometer (Cu $K\alpha$ radiation). The cell parameters for LaCoAsO were refined using least-squares fitting of the measured peak positions in 2θ=20°–70° using JADE 6.1 MDI package.

Neutron powder-diffraction data on $LaFe_{1-x}Co_xAsO$ with x=0, 0.11, and 0.15 were collected on the C2 diffractometer[36] operated by the Neutron Program for Materials Research of the National Research Council of Canada. Each sample of 1–2 g was placed in a helium-filled vanadium can that was sealed with an indium gasket. Data were collected at two different wavelengths of 1.330910 and 2.372630 Å. For x=0 and 0.15, powder-diffraction data were collected at 4 and also 300 K. For x=0.11, data were collected at 4, 10, 15, 30, 50, 100, 150, 200, and 300 K.

TABLE II. Crystallographic data of $LaFe_{1-x}Co_xAsO$: x=0.11.

T (K)	4		300
Space group	*P*4/*nmm*		*P*4/*nmm*
a (Å)	4.02771(1)		4.0351(1)
b (Å)	$=a$		$=a$
c (Å)	8.6860(3)		8.7132(3)
V (Å^3)	140.908(6)		141.871(11)
Z	2		2
d range (Å)		0.8–10.6	
wR_p	3.38		3.61
χ^2	3.94		4.25
Atomic parameters:			
La	$2c(\frac{1}{4},\frac{1}{4},z)$, z=0.1412(3) U_{iso}=0.0038(8) Å^2		$2c(\frac{1}{4},\frac{1}{4},z)$, z=0.1412(3) U_{iso}=0.0049(9) Å^2
Fe/Co	$2b(\frac{3}{4},\frac{1}{2},z)$, U_{iso}=0.0015(8) Å^2		$2b(\frac{3}{4},\frac{1}{2},\frac{1}{2})$, U_{iso}=0.0087(11) Å^2
As	$2c(\frac{1}{4},\frac{1}{4},z)$, z=0.6502(3) U_{iso}=0.0012(9) Å^2		$2c(\frac{1}{4},\frac{1}{4},z)$, z=0.6505(4) U_{iso}=0.0054(12) Å^2
O	$2a(\frac{3}{4},\frac{1}{4},0)$, U_{iso}=0.0057(11) Å^2		$2a(\frac{3}{4},\frac{1}{4},0)$, U_{iso}=0.0057(14) Å^2

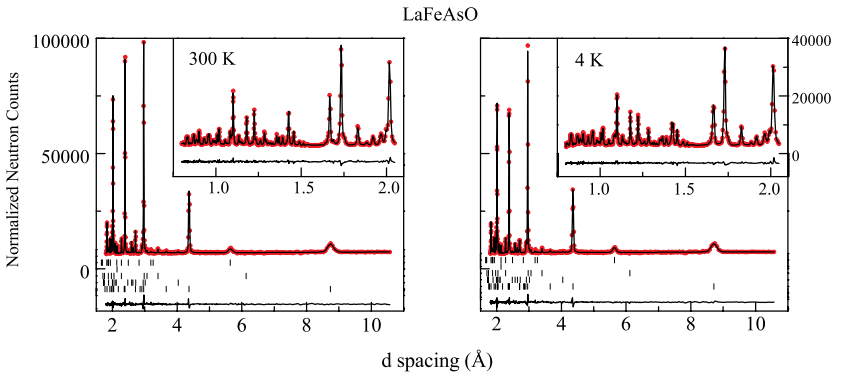

FIG. 2. (Color online) Refined neutron powder-diffraction for LaFeAsO at 4 K and 300 K. The tick marks are bottom to top: main phase in *Cmma* (left), *P*4/*nmm* (right) at 81.6%; FeAs at 7.9%; La_2O_3 at 9.2%; V; and $La(OH)_3$ at 1.3%.

Neutron powder-diffraction data for both wavelengths were jointly refined for the main and impurity phases of FeAs and La_2O_3 using GSAS (Refs. 37 and 38) with the EXPGUI (Ref. 39) interface. For all the refinements, the pseudo-Voigt function (profile function 3 in GSAS) was used and both Lorentzian and Gaussian widths were allowed to vary. Zero-point parameter was also allowed to change. The background was modeled using a ten-term Chebyshev polynomial function. The lattice parameters for the main as well as impurity phases were refined. Isotropic thermal parameters and fractional coordinates were refined for all the atoms in the primary phase. For $x=0.11$ and 0.15 samples, a single thermal parameter was used for both Fe and Co and the occupancy factors were refined with the constraint that they add up to the full occupancy of the site. The details of the neutron powder refinement conditions and the atomic parameters at 4 or 300 K for *d* range of 0.8 to 10.6 Å are given in Tables I and II for $x=0$ and 0.11, respectively.

Powder x-ray diffraction patterns were collected at beamline X16C of the National Synchrotron Light Source utilizing x rays of wavelength 0.69869 Å from a Si(111) channel-cut monochromator and a Ge(111) analyzer. The data for $LaFe_{1-x}Co_xAsO$ with $x=0.05$, 0.11, 0.2, and 0.5 were collected at room temperature. Samples were ground in air and diluted with ground glass wool and flame sealed in 1 mm capillaries. Total exposure to the atmosphere before sealing was approximately 1 min for each sample. Capillaries were spun during data collection to improve counting statistics. The high-resolution x-ray data were modeled in a similar fashion as the neutron data described above.

dc magnetization was measured as a function of temperature and field using a Quantum Design magnetic property measurement system. For a temperature sweep experiment, the sample was cooled to 1.8 K in zero-field (zfc) and data were collected by warming from 1.8 to 300 K in an applied field. The sample was then cooled in the applied field (fc) and the measurement was repeated from 1.8 K. The magnetic-susceptibility results are presented per mole of $LaFe_{1-x}Co_xAsO$ ($0 \leq x \leq 1$) formula unit (cm^3/mol). Electrical resistivity, Seebeck coefficient, and specific-heat measurements were obtained using a Quantum Design physical property measurement system. For dc resistance measurements, electrical contacts were placed on samples in standard four-probe geometry using Pt wires and silver epoxy (EPOTEK H20E). Gold-coated copper leads were used for Seebeck coefficient measurements.

III. RESULTS AND DISCUSSION

A. Structure

For $LaFe_{1-x}Co_xAsO$, neutron-diffraction data were collected on $x=0$, 0.11, 0.15, while x-ray diffractions were done on $x=0.05$, 0.11, 0.2, and 0.5 compositions.

The structure of $LaFe_{1-x}Co_xAsO$ at 300 K for all compositions of *x* was refined with the tetragonal space group *P*4/*nmm* (No. 129, origin choice 2; *Z*=2) (Refs. 14 and 15) (Fig. 1). La and As atoms are located at Wyckoff positions

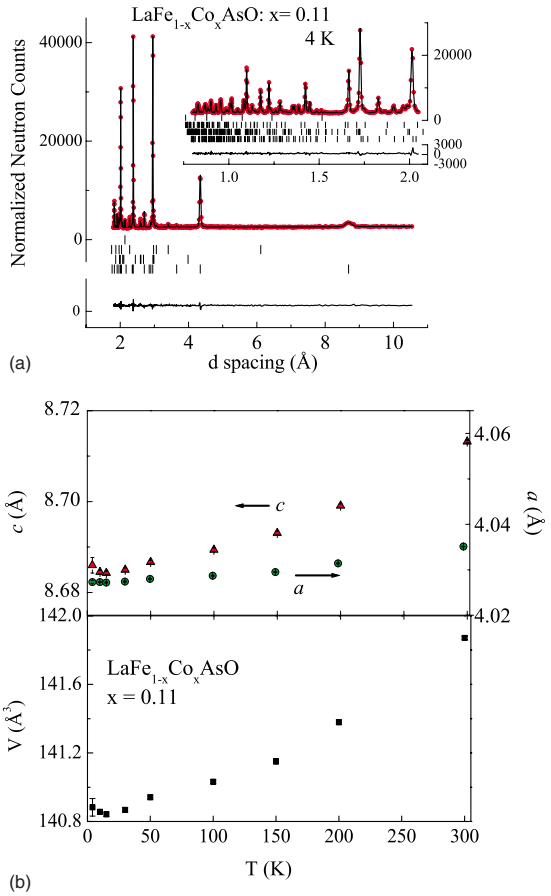

FIG. 3. (Color online) For $LaAsFe_{1-x}Co_xO$, $x=0.11$. (a) the refined neutron powder-diffraction profile at 4 K and (b) the change in lattice parameters and cell volume with temperature. The tick marks in (a) are bottom to top: main phase in *P*4/*nmm*, FeAs, La_2O_3, and V.

TABLE III. Bond distances as a function of temperature for $LaFe_{1-x}Co_xAsO$: $x=0$ and $x=0.11$.

$LaAsFe_{1-x}Co_xO$: $x=0.11$					
T (K)	Fe-As (Å)	La-As (Å)	La-O (Å)	Fe-O (Å)	Fe-Fe (Å)
4	2.408(5)	3.3741(31)	2.351(4)	4.3430(9)	2.8478(3)
10	2.4024(25)	3.3738(15)	2.3559(19)	4.3423(2)	2.8477(1)
15	2.4028(25)	3.3739(15)	2.3552(19)	4.3421(2)	2.8476(1)
30	2.4019(25)	3.3745(15)	2.3559(19)	4.3425(2)	2.8478(1)
50	2.4023(25)	3.3756(15)	2.3558(20)	4.3434(2)	2.8482(1)
100	2.4024(25)	3.3776(15)	2.3555(19)	4.3447(2)	2.8487(2)
200	2.4044(26)	3.3799(15)	2.3576(20)	4.3495(2)	2.8506(1)
300	2.4110(5)	3.3832(31)	2.356(4)	4.3555(9)	2.8528(3)
LaFeAsO					
4	2.4017(19)	3.3791(11)	2.3650(14)	4.3558(2)	2.8412(1), 2.8551(1)
300	2.4049(20)	3.3836(12)	2.3682(16)	4.3693(2)	2.8528(1)

$2c$, O site is at $2a$, while Fe/Co may be shared at site $2b$. For LaFeAsO, the lattice constants obtained from neutron data were $a=4.0345(1)$ Å and $c=8.7387(4)$ Å (see Fig. 2) and compare well with the reported $a=4.038(1)$ Å and $c=8.753(6)$ Å.[15] The incorporation of Co in $x=0.11$ in the Fe site reduces the cell volume by 0.26% due to contraction of the lattice constant c[=8.7132(3) Å]. For F-doped $LaFeAsO_{1-x}F_x$ with $x=0.11$, the lattice constants are found to shrink by 0.17% [4.0277(2) Å] and 0.30% [8.7125(4) Å], respectively.[2]

The structure of LaFeAsO at 4 K was refined with orthorhombic space group *Cmma* (No. 67; $Z=4$), earlier reported at 120 K by Nomura *et al.*[18] As a result of this phase transition, the a- and b-crystallographic axes rotate by 45°. Splitting of several reflections of the room-temperature tetragonal phase (111,112,322) was observed at 150 K as the temperature was lowered to 4 K. The atoms in this low-temperature orthorhombic phase are characterized by the same coordination as that of tetragonal structure. La and As atoms are located on Wyckoff positions $4g$, Fe on $4b$, and O on $4a$.

For $LaFe_{1-x}Co_xAsO$ with $x=0.11$, similar peak splitting to LaFeAsO was, however, not observed in the diffraction data down to 4 K. The data was refined within the tetragonal $P4/nmm$ framework, comparable to that for 14% F-doped LaFeAsO structure at 120 K.[18] The refined neutron-diffraction pattern at 4 K is shown in Fig. 3(a). The data were refined for the main (89.8%) and impurity phases of FeAs (4.1%) and La_2O_3 (6.1%).

For $x=0.11$, the temperature dependence of lattice parameters and the cell volumes are shown in Fig. 3(b). The a and c parameters seem to vary nonlinearly with increasing temperature and by 0.18% and 0.31%, respectively, over the 4 to 300 K region; the cell volume change is 0.68%. It has been suggested that the R-As distance and Fe-As-Fe angle are the two crucial parameters in the structure of RFeAsO that control the effective bandwidths in these materials and, hence,

TABLE IV. Two selected sets of bond angles as a function of temperature for $LaFe_{1-x}Co_xAsO$:$x=0$ and $x=0.11$.

$LaAsFe_{1-x}Co_xO$: $x=0.11$		
T (K)	Fe-As-Fe	O-La-O
4	113.5(4), 72.51(18)	117.86(34), 74.55(15)
10	113.90(18), 72.70(9)	117.46(15), 74.37(7)
15	113.86(18), 72.68(9)	117.51(15), 74.39(7)
30	113.93(19), 72.71(9)	117.46(15), 74.37(7)
50	113.94(19), 72.71(9)	117.50(16), 74.39(7)
100	113.96(18), 72.72(9)	117.56(15), 74.42(7)
200	113.93(19), 72.71(9)	117.51(16), 74.39(7)
300	113.6(4), 72.73(9)	117.81(35), 74.53(16)
LaFeAsO		
4	113.97(14), 72.52(7), 72.94(7)	116.76(11), 74.26(5), 73.83(5)
300	114.02(15),72.76(7)	116.82(12),74.07(6)

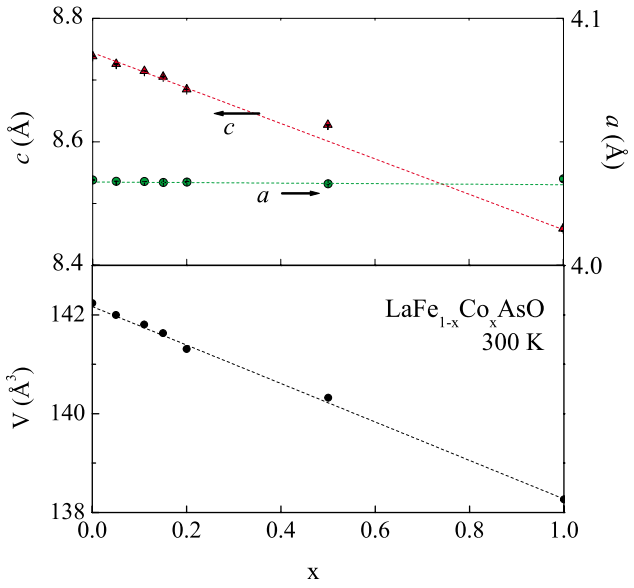

FIG. 4. (Color online) Refined lattice parameters and cell volume for $LaAsFe_{1-x}Co_xO$ for $0 \leq x \leq 1$ at 300 K.

the superconductivity.[40] At 300 K, the variation of the bond distance and angle of the $x=0.11$ versus Fe parent[41] (Tables III and IV)[FG] is very small (La-As: 0.06%; Fe-As-Fe: 0.05%). However, these differences are significantly larger at 4 K (La-As: 0.11%; Fe-As-Fe: −0.14%). It is interesting to note that the large distortion of the $FeAs_4$ tetrahedron in $x=0.11$ is accompanied by a similarly large distortion in La_4O tetrahedron, whereas F doping in the LaO layer in LaFeAsO causes no distortion in $FeAs_4$ tetrahedron.[40] F doping in the La_4O layer changes the Fe-As bond only slightly; however, Co doping in the $FeAs_4$ layer changes the La-O bond significantly (Table III).

The occupancy of Co on Fe $2b$ site refines as $LaFe_{0.92(1)}Co_{0.08(1)}AsO$ for $x=0.11$. Also, the average occupancy of Co for nominally prepared $x=0.15$ sample refines as $x=0.12(1)$. Assuming a linear dependence between nominal x and the Co concentration, the $x=0.05$, 0.2, and 0.5 samples are likely to have ~4%, 16%, and 40% cobalt. Despite the variance between the nominal and measured compositions, they will continue to be presented with their nominal x values. The three compositions are stoichiometric in oxygen content as $2a$ site was refined to unity at every temperature that the data were collected.

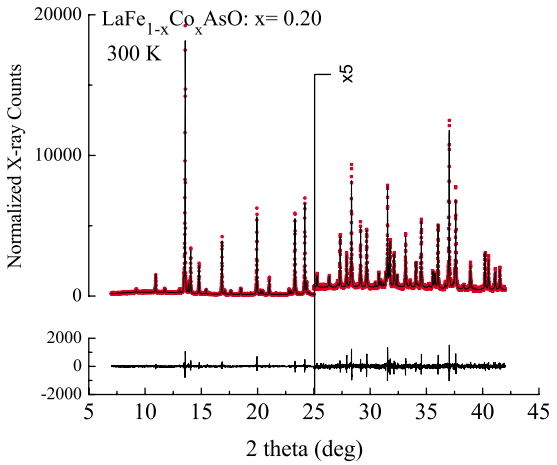

FIG. 5. (Color online) Refined x-ray powder-diffraction profile for $LaAsFe_{1-x}Co_xO$ with $x=0.2$ at 300 K. The tick marks from bottom to top: main phase in $P4/nmm$ (89.2%); FeAs (3.6%); and La_2O_3 (7.2%).

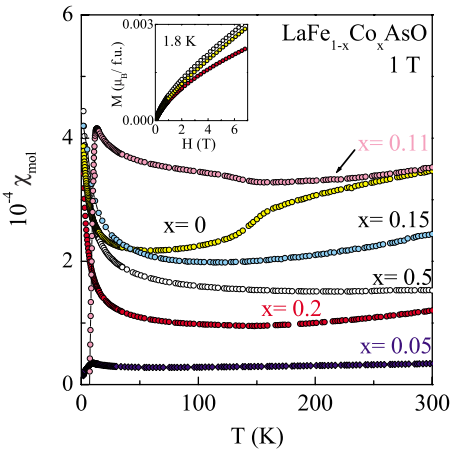

FIG. 6. (Color online) The dependence of molar susceptibility in zero field in $LaAsFe_{1-x}Co_xO$ for $0 \leq x \leq 0.5$. The field dependent magnetization at 1.8 K for the nonsuperconducting compositions (inset).

From $x=0$ to 1, the reduction in the a and c parameters and cell volumes are 0.04%, 3.20%, and 2.79%, respectively (Fig. 4). It was suggested that the T_c in $RFeAsO_{1-y}$ is strongly dependent on the tetrahedral distortion represented by As-Fe-As bond angle.[41] We also observe similar trend from our x-ray data at various concentration of Co. From $x=0.11$ to 0.2, As-Fe-As bond angle decreases from 107.35° to 106.99° (see Fig. 5). It should be mentioned here that at $x=0.2$, superconductivity is lost (Sec. III B).

B. Physical properties

The temperature dependence of molar magnetic susceptibility in 1 T for the $LaFe_{1-x}Co_xAsO$ system is shown in Fig. 6. For $0 \leq x \leq 0.5$, χ values vary between 3×10^{-5} and 3.5×10^{-4} cm^3/mol at 300 K. These values are smaller than that reported for $LaFeAsO_{0.89}F_{0.11}$ (1.8×10^{-3} cm^3/mol at 300 K and 0.1 T).[2] For LaFeAsO (Fig. 6), magnetic susceptibility decreases with decreasing temperature, with an anomaly at ~150 K and a rise below 50 K. For $x=0.2$ and 0.5, χ is weakly temperature dependent with a gradual increase below 50 K. The field-dependent magnetization data for $x=0$, 0.2, and 0.5 are shown in the inset of Fig. 6 and none of the samples approach saturation at 7 T, reaching <0.003 μ_B/f.u.

The temperature dependence of magnetization in 1 T for LaCoAsO is shown in Fig. 7(a). The $M(T)$ increases below ~80 K, indicating possible ferromagnetic ordering. The inset of Fig. 7(a) shows a plot of the inverse magnetization and the fit to a Curie-Weiss law, where $M/H \approx \chi = C/(T-\theta) + \chi_o$; C is the Curie constant, θ is the paramagnetic Weiss temperature, and χ_o is a temperature-independent term. The fit was

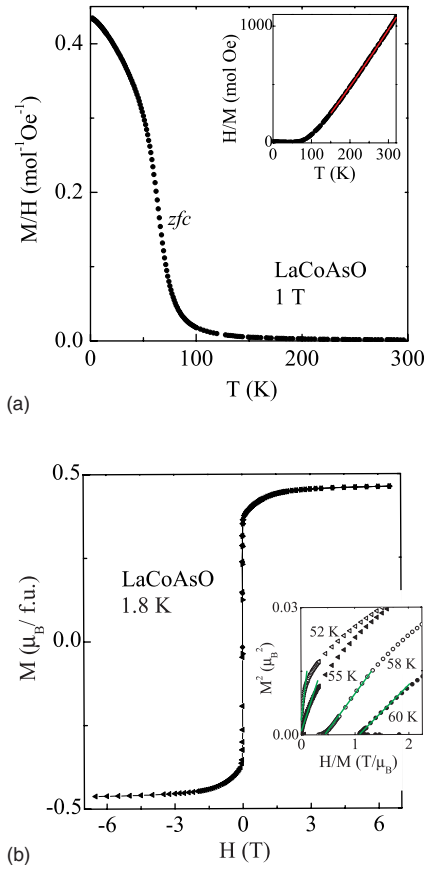

FIG. 7. (Color online) (a) Temperature dependence of molar susceptibility at 1 T for LaCoAsO. The plot of the inverse molar susceptibility with fit to modified Curie-Weiss above 150 K in red (dark gray) line (inset). (b) Magnetization versus applied field at 1.8 K for LaCoAsO. The Arrott plots in the form of M^2 versus H/M at temperatures in the vicinity of magnetic transition (inset).

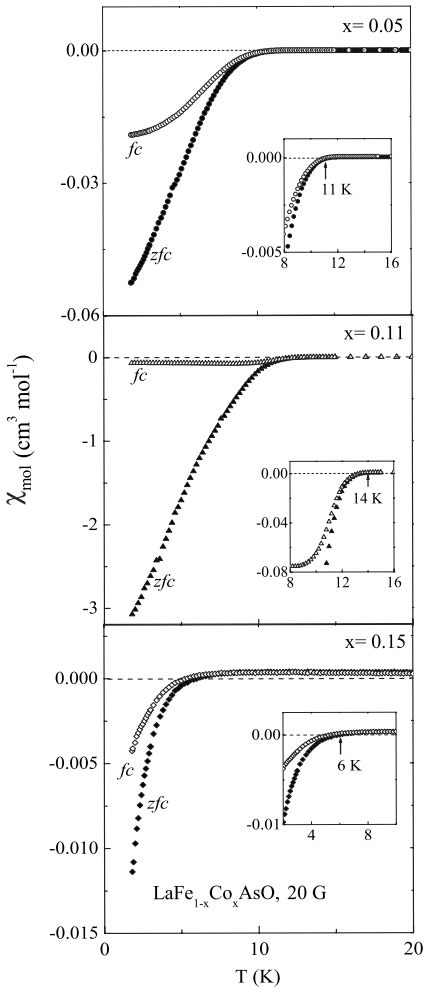

FIG. 8. Temperature dependence of molar susceptibility in zero-field cooled (zfc) (filled symbols) and field cooled (fc) (open symbols) for $LaFe_{1-x}Co_xAsO$ in 20 Oe for $x=0.05$ (top), 0.11 (middle), and 0.15 (bottom). The enlarged regions around T_c are shown in the insets.

done for $T>150$ K. Assuming Co is the only moment-bearing ion, then the term C is related to the effective moment in paramagnetic state and the theoretically expected 3.87 μ_B ($S=3/2$). Experimentally, the Curie-Weiss fit gives $\mu_{\text{eff}} \approx 1.4$ μ_B per Co. This result is comparable to that recently reported for LaCoAsO.[42] The Weiss temperature is positive and $\theta \approx 90$ K; $\chi_o \approx -6\times10^{-6}$/mol. Field-dependent magnetization data, $M(H)$, at 1.8 K are shown in Fig. 7(b). The magnetization rises rapidly up to ~500 G and changes weakly thereafter. The precipitous rise in magnetization at low fields again suggests ferromagnetism. An applied field of ~5 T gives 0.46 μ_B/f.u.; this field is insufficient to saturate the magnetization data to 3 μ_B/Co^{2+} as expected for localized high-spin Co^{2+} ions.

In order to locate the ferromagnetic transition, magnetization isotherms in the vicinity of Curie temperatures have been measured for the construction of Arrott plots[43] in the form of M^2 versus HM^{-1} [Fig. 7(b), inset]; for this sample, $55<T_c<58$ K. This range of T_c is slightly lower than that reported earlier.[1,42] Despite the suggestion of a ferromagnetic component in magnetization measurements, there is lack of anomaly in specific heat on several different polycrystalline samples. One scenario that may explain the data is that LaCoAsO is a quasi-2D itinerant metal with strong in-plane ferromagnetic interactions but extremely weak out-of-plane interactions. In this scenario, LaCoAsO would be a strongly exchange-enhanced paramagnet and that application of even a small field produces a large ferromagnetic response.

Figure 8 shows the temperature dependence of magnetic susceptibility, measured under zfc and fc conditions at 20 Oe for $LaFe_{1-x}Co_xAsO$ with $x\leq0.15$. The susceptibility becomes negative below ~11, 14, and 6 K for $x=0.05$, 0.11, and 0.15, respectively. Assuming theoretical density of roughly 6.68 g/cm^3 and χ value of the perfect diamagnetism, we estimate the shielding fraction about 15% and Meissner fraction near 6% at 2 K for $x=0.05$. Although $x=0.11$ has higher T_c value and higher shielding fraction (90%), the Meissner fraction is only about 2%. For $x=0.15$, both the shielding and Meissner fractions are less than 1%. It should be noted that since the Meissner fraction is determined by pinning and penetration effects, its interpretation is ambiguous on sintered samples.

Figure 9(a) shows the temperature dependence of the electrical resistivity (ρ) in zero field. Similar to the other reports for LaFeAsO,[5,8] $\rho_{300\text{ K}} \approx 4$ mΩ cm, then it increases

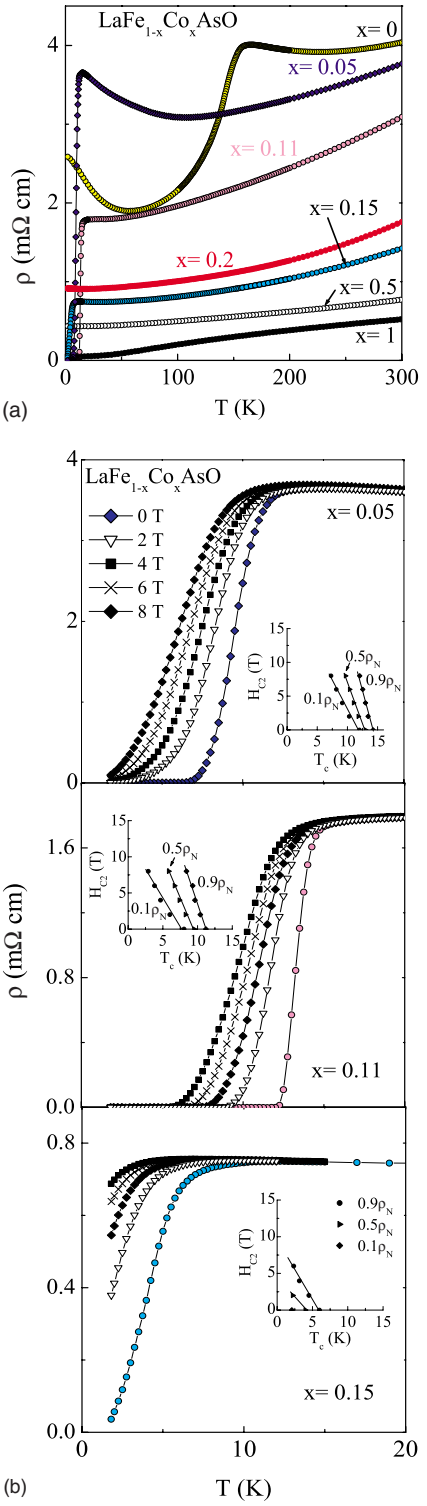

FIG. 9. (Color online) (a) Temperature dependence of resistivity for $LaFe_{1-x}Co_xAsO$ for $0 \leq x \leq 1$. (b) Temperature dependence of resistivity at various applied fields for $x=0.05$ (top), 0.11 (middle), and 0.15 (bottom). For each composition, the upper critical field H_{c2} is found from 90%, 50%, and 10% estimates of the normal-state value ρ_N and plotted versus critical temperature as insets.

slightly with decreasing temperature peaking at ~160 K. This upturn in ρ is likely associated with the increased charge-carrier scattering by lattice fluctuations related to the

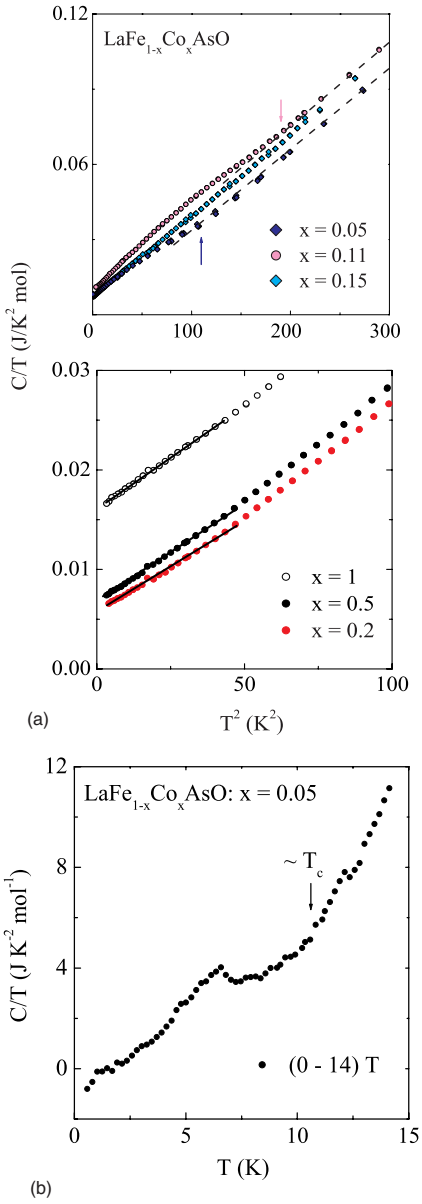

FIG. 10. (Color online) (a) For $LaFe_{1-x}Co_xAsO$ and $0.05 \leq x \leq 1$, temperature dependence of specific heat in the form of C/T versus T^2 below ~17 K (top) and 10 K (bottom). Anomalies are shown by arrows for $x=0.05$ and 0.11. For $0.2 \leq x \leq 1$ (bottom), linear fits are below ~6 K. (b) For $LaFe_{1-x}Co_xAsO$ and $x=0.05$, the temperature dependence of the subtracted 0 T from 14 T specific-heat data. The arrow shows the onset of the deviation from the background at $\sim T_c$.

onset of the structural transition. The samples with $x=0.05$, 0.11, and 0.15 exhibit superconductivity. Higher doping levels of $x=0.2$, 0.5, and 1 give only metallic behavior. The electrical conductivity increases by a factor of 8 from LaFeAsO ($3d^6$) to LaCoAsO ($3d^7$).

The resistive transitions for the superconducting compositions shift to lower temperatures by applying a magnetic field [Fig. 9(b)]. The transition width for each sample becomes wider with increasing H, a characteristic of type-II superconductivity. Here we define a transition temperature $T_c(H)$, which satisfies the condition that $\rho(T_c,H)$ equals a

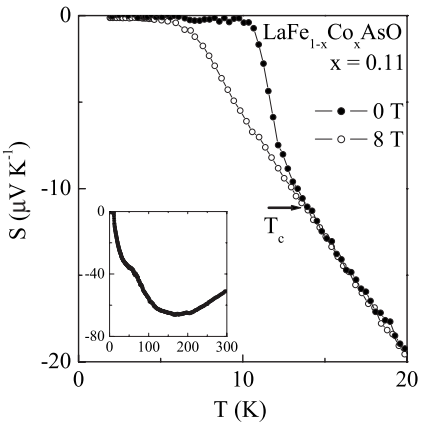

FIG. 11. Temperature dependence of Seebeck coefficient for $LaFe_{1-x}Co_xAsO$ with $x=0.11$ in applied fields of 0 and 8 T. Inset is zero-field result up to room temperature.

fixed percentage of the normal-state value (ρ_N) for each field H. The $T_c(H)$ values for $\rho=10$, 50, and 90% are shown as insets of Fig. 9(b) represented by the upper critical field $H_{c2}(T)$. In all cases we find that $H_{c2}(T)$ has a linear dependence with no sign of saturation. T_c at zero field for $0.1\rho_N$ are 11.2, 14.3, and 6.0 K for $x=0.05$, 0.11, and 0.15, respectively. The transition width $\Delta T_c=T_c(90\%)-T_c(10\%)$ are 3.2, 2.3, and 3.9 K, respectively. The ΔT_c values are smaller than the reported 4.5 K for $LaFeAsO_{0.89}F_{0.11}$ with $T_c^{\text{onset}}=28.2$ K.[2]

Figure 10(a) shows the temperature dependence of specific heat in the form of C/T versus T^2 from 1.8 to 20 K. For each $x=0.05$ and 0.11, there is clearly a broad specific-heat anomaly below $\sim T_c$. For $x=0.2$, 0.5, and 1 samples, the C/T vs T^2 plot is linear between ~ 2 and 6 K [Fig. 10(a), bottom]. This allows the estimation of electronic γ and lattice β values as $C=\gamma T+\beta T^3$. The fits yield γ in units of mJ/(K^2 mol atom) for $x=0.2$, 0.5, and 1, respectively, as 1.405(1), 1.68(1), and 4.02(1). The value of the Debye temperature (θ_D) was subsequently calculated in the low-temperature limit ($\beta=12\pi^4R/5\theta^3$) and $\theta_D=342(9)$K for these samples. This value is comparable to the Debye temperature of ≈ 280 K for LaFeAsO (Ref. 5) and ≈ 325 K for $LaFeAsO_{0.89}F_{0.11}$.[2]

For $x=0.05$, the specific heat under magnetic fields of 14 T was measured and subtracted from zero-field data. Figure 10(b) gives the temperature dependence of $\Delta C/T$ data and illustrates a deviation from high-temperature behavior below $T_c\sim 11$ K, peaking at 7 K. The broadened transition reflects the inhomogeneity of superconducting phase, likely due to the random Co distribution. Nevertheless, the observation of specific-heat anomaly at T_c indicates bulk superconductivity in the discovered Co-doped LaFeAsO. The origin of the field dependence of the background is not understood and has yet to be investigated.

The Seebeck coefficient S of $LaFe_{1-x}Co_xAsO$ with $x=0.11$ at 0 T is shown in the inset of Fig. 11. S is negative over the entire temperature range, indicating dominant electron conduction. This result is similar to F doping ($x=0.11$) in LaFeAsO and provides evidence for electron doping.[2] S varies from -50 μV/K at 300 K to a value of ~ -65 μV/K at ~ 160 K then decreases in magnitude as the temperature is lowered further. The maximum in the data is probably due to the competition between dominant electronlike bands and the expected proximity of holelike bands near the Fermi energy. Figure 11 gives the magnetic-field effect below 25 K; T_c at ~ 14 K is clearly suppressed at 8 T.

IV. CONCLUSIONS

In this work we report the synthesis, structure, magnetization, resistivity, specific heat, and Seebeck coefficient of $LaFe_{1-x}Co_xAsO$ for several values of x. The most important observation is that Co acts as an effective dopant and produces superconductivity in this system. In most respects, $LaFe_{1-x}Co_xAsO$ behaves similarly to $LaFeAsO_{1-x}F_x$ but with a smaller T_c. This is likely due to the stronger effects of disorder produced by doping in the FeAs layers rather than in the LaO layers. It is actually somewhat surprising that the superconductivity in $LaFe_{1-x}Co_xAsO$ is quite robust to in-plane disorder and this behavior will need to be understood as part of a comprehensive theory of the superconducting mechanism.

ACKNOWLEDGMENTS

We would like to thank D. J. Singh for helpful discussions. The research at ORNL was sponsored by the Division of Materials Sciences and Engineering, Office of Basic Energy Sciences, and the U.S. Department of Energy. L.M.D.C. would like to thank CNBC NRC technicians, R. Sammon, D. Dean, and T. Dodd for the setup of the closed cycle refrigeration system used for the neutron-diffraction measurements.

[1] Y. Kamihara, T. Watanabe, M. Hirano, and H. Hosono, J. Am. Chem. Soc. **130**, 3296 (2008).
[2] A. S. Sefat, M. A. McGuire, B. C. Sales, R. Jin, J. Y. Howe, and D. Mandrus, Phys. Rev. B **77**, 174503 (2008).
[3] F. Hunte, J. Jaroszynski, A. Gurevich, D. C. Larbalestier, R. Jin, A. S. Sefat, M. A. McGuire, B. C. Sales, D. K. Christen, and D. Mandrus, Nature (London) **453**, 903 (2008).
[4] I. Mazin, D. Singh, M. Johannes, and M. Du, Phys. Rev. Lett. **101**, 057003 (2008
[5] J. Dong *et al.*, Europhys. Lett. **83**, 27006 (2008).
[6] X. L. Wang, R. Ghorbani, G. Peleckis, and S. X. Dou, arXiv:0806.0063 (unpublished).
[7] H.-H. Klauss, H. Luetkens, R. Klingeler, C. Hess, F. Litterst, M. Kraken, M. M. Korshunov, I. Eremin, S.-L. Drechsler, R. Khasanov, A. Amato, J. Hamann-Borreo, N. Leps, A. Kondrat, G. Behr, J. Werner, and B. Buchner, arXiv:0805.0264 (unpublished).
[8] M. A. McGuire, A. D. Christianson, A. S. Sefat, B. C. Sales, M.

D. Lumsden, R. Jin, E. A. Payzant, D. Mandrus, Y. Luan, V. Keppens, V. Varadarajan, J. W. Brill, R. P. Hermann, M. T. Sougrati, F. Grandjean, and G. J. Long, arXiv:0806.3878 (unpublished).

[9] K. Kuroki, S. Onari, R. Arita, H. Usui, Y. Tanaka, H. Kontani, and H. Aoki, arXiv:0803.3325 (unpublished).

[10] H. Eschrig, arXiv:0804.0186 (unpublished).

[11] P. A. Lee, N. Nagaosa, and X.-G. Wen, Rev. Mod. Phys. **78**, 17 (2006).

[12] R. J. Birgeneau, C. Stock, J. M. Tranquada, and K. Yamada, J. Phys. Soc. Jpn. **75**, 111003 (2006).

[13] V. Johnson and W. Jeitschko, J. Solid State Chem. **11**, 161 (1974).

[14] B. I. Zimmer, W. Jeitschko, J. H. Albering, R. Glaum, and M. Reehuis, J. Alloys Compd. **229**, 238 (1995).

[15] P. Quebe, L. J. Terbüchte, and W. Jeitschko, J. Alloys Compd. **302**, 70 (2000).

[16] D. J. Singh and M. H. Du, Phys. Rev. Lett. **100**, 237003 (2008).

[17] C. de la Cruz, Q. Huang, J. W. Lynn, J. Li, W. Ratcliff, J. L. Zarestky, H. A. Mook, G. F. Chen, J. L. Luo, N. L. Wang, and P. Dai, Nature (London) **453**, 899 (2008).

[18] T. Nomura, S. W. Kim, Y. Kamihara, M. Hirano, P. V. Sushko, K. Kato, M. Takata, A. L. Shluger, and H. Hosono, arXiv:0804.3569 (unpublished).

[19] J. P. Carlo, Y. J. Uemura, T. Goko, G. J. MacDougall, J. A. Rodriguez, W. Yu, G. M. Luke, P. Dai, N. Shannon, S. Miyasaka, S. Suzuki, S. Tajima, G. F. Chen, W. Z. Hu, J. L. Luo, and N. L. Wang, arXiv:0805.2186 (unpublished).

[20] G. Giovannetti, S. Kumar, and J. van den Brink, arXiv:0804.0866, J. Phys. B (to be published).

[21] F. Ma and Z.-Y. Lu, Phys. Rev. B **78**, 033111 (2008).

[22] C. Cao, P. J. Hirschfeld, and H.-P. Cheng, Phys. Rev. B **77**, 220506(R) (2008).

[23] W. Lu, J. Yang, X. L. Dong, Z. A. Ren, G. C. Che, and Z. X. Zhao, New J. Phys. **10**, 063026 (2008).

[24] S. Kitao, Y. Kobayashi, S. Higashitaniguchi, M. Saito, Y. Kamihara, M. Hirano, T. Mitsui, H. Hosono, and M. Seto, arXiv:0805.0041 (unpublished).

[25] Z.-A. Ren, J. Yang, W. Lu, W. Yi, X.-L. Shen, Z.-C. Li, G.-C. Che, X.-L. Dong, L.-L. Sun, F. Zhou, and Z.-X. Zhao, Europhys. Lett. **82**, 57002 (2008).

[26] X. H. Chen, T. Wu, G. Wu, R. H. Liu, H. Chen, and D. F. Fang, Nature (London) **453**, 761 (2008).

[27] P. Cheng, L. Fang, H. Yang, X.-Y. Zhu, G. Mu, H.-Q. Luo, Z.-S. Wang, and H.-H. Wen, Sci. China, Ser. G **51**, 719 (2008).

[28] R. H. Liu, G. Wu, T. Wu, D. F. Fang, H. Chen, S. Y. Li, K. Liu, Y. L. Xie, X. F. Wang, R. L. Yang, C. He, D. L. Feng, and X. H. Chen, arXiv:0804.2105 (unpublished).

[29] G. F. Chen, Z. Li, D. Wu, G. Li, W. Hu, J. Dong, P. Zheng, J. L. Luo, and N. L. Wang, Phys. Rev. Lett. **100**, 247002 (2008).

[30] R. Zhi-An, L. Wei, Y. Jie, Y. Wei, S. Xiao-Li, L. Zheng-Cai, C. Guang-Can, D. Xiao-Li, and S. Li-Ling, Chin. Phys. Lett. **25**, 2215 (2008).

[31] C. Wang, L. Li, S. Chi, Z. Zhu, Z. Ren, Y. Li, Y. Wang, X. Lin, Y. Luo, S. Jiang, X. Xu, G. Cao, and Z. Xu, arXiv:0804.4290 (unpublished).

[32] H.-H. Wen, G. Mu, L. Fang, H. Yang, and X. Zhu, Europhys. Lett. **82**, 17009 (2008).

[33] Z.-A. Ren, J. Yang, W. Lu, W. Yi, G.-C. Che, X.-L. Dong, L.-L. Sun, and Z.-X. Zhao, Europhys. Lett. **83**, 17002 (2008).

[34] H. Kito, H. Eisaki, and A. Iyo, J. Phys. Soc. Jpn. **77**, 063707 (2008).

[35] J. Yang, Z.-C. Li, W. Lu, W. Yi, X.-L. Shen, Z.-A. Ren, G.-C. Che, X.-L. Dong, L.-L. Sun, F. Zhou, and Z.-X. Zhao, Supercond. Sci. Technol. **21**, 082001 (2008).

[36] L. M. D. Cranswick, R. Donaberger, I. P. Swainson, and Z. Tun, J. Appl. Crystallogr. **41**, 373 (2008).

[37] A. C. Larson and R. B. Von Dreele, General Structure Analysis System (GSAS).

[38] Los Alamos National Laboratory Report No. LAUR 86-748, 1987.

[39] B. H. Toby, J. Appl. Crystallogr. **34**, 210 (2001).

[40] J. Zhao, Q. Huang, C. de la Cruz, S. Li, J. W. Lynn, Y. Chen, M. A. Green, G. F. Chen, G. Li, Z. Li, J. L. Luo, N. L. Wang, and P. Dai, arXiv:0806.2528 (unpublished).

[41] C.-H. Lee, T. Ito, A. Iyo, H. Eisaki, H. Kito, M. T. Fernandez-Diaz, K. Kihou, H. Matsuhata, M. Braden, and K. Yamada, J. Phys. Soc. Jpn. **77**, 083704 (2008).

[42] H. Yanagi, R. Kawamura, T. Kamiya, Y. Kamihara, M. Hirano, T. Nakamura, H. Osawa, and H. Hosono, Phys. Rev. B **77**, 224431 (2008).

[43] A. Arrott, Phys. Rev. **108**, 1394 (1957).